



An experimental investigation of eco-friendly treated GNP heat transfer growth: circular and square conduit comparison

O. Almatar AbdRabbuh¹ · C. S. Oon² · S. N. Kazi¹ · A. H. Abdelrazek¹ · Waqar Ahmed^{1,3} · A. R. Mallah¹ · A. Badarudin¹ · Irfan Anjum Badruddin⁴ · Sarfaraz Kamangar⁴

Received: 6 October 2019 / Accepted: 28 March 2020 / Published online: 23 April 2020
© Akadémiai Kiadó, Budapest, Hungary 2020

Abstract

This paper presents the results of bio-based functionalized nanofluids on heat transfer and pressure drop investigation in square and circular tube heat exchangers to obtain enhanced heat dissipation. Graphene nanoplatelet (GNP) was covalently functionalized with the clove bud extractions. At different concentrations of graphene in nanofluid, the results showed higher thermal conductivity with the rising of the suspension concentrations. The nanofluid was compared with the traditional working fluid (water), and the result showed higher thermal conductivity and improved heat transfer coefficient. The present experimental investigation focused on the performance of heat transfer, thermophysical properties and pressure drop of GNP-based water nanofluid in different configurations of heat exchanger tubes. Substantial improvement in the rate of heat transfer with the loading of well-dispersed GNPs in the base fluid was observed. The nanofluid enhances the heat transfer coefficient irrespective of the circular or square flow passage configurations. Furthermore, the heat transfer coefficient enhanced with the increase in concentrations of the nanoparticles in the fluid and the pressure loss increment was much less relative to the gain in heat transfer. The Nusselt number in the circular test section was higher than that in the square test section. Thus, the GNP water-based nanofluids emerged as a potential high-performance heat exchanging liquid utilizing circular flow passage.

Keywords Turbulent flow · Heat transfer coefficient · Clove bud · Graphene nanoplatelets · Eco-friendly

Electronic supplementary material The online version of this article (<https://doi.org/10.1007/s10973-020-09652-5>) contains supplementary material, which is available to authorized users.

✉ C. S. Oon
oonsean2280@yahoo.com

✉ S. N. Kazi
salimnewaz@um.edu.my

¹ Department of Mechanical Engineering, Faculty of Engineering, University of Malaya, 50603 Kuala Lumpur, Malaysia

² School of Engineering, Mechanical Engineering Discipline, Monash University Malaysia, Jalan Lagoon Selatan, 47500 Bandar Sunway, Selangor Darul Ehsan, Malaysia

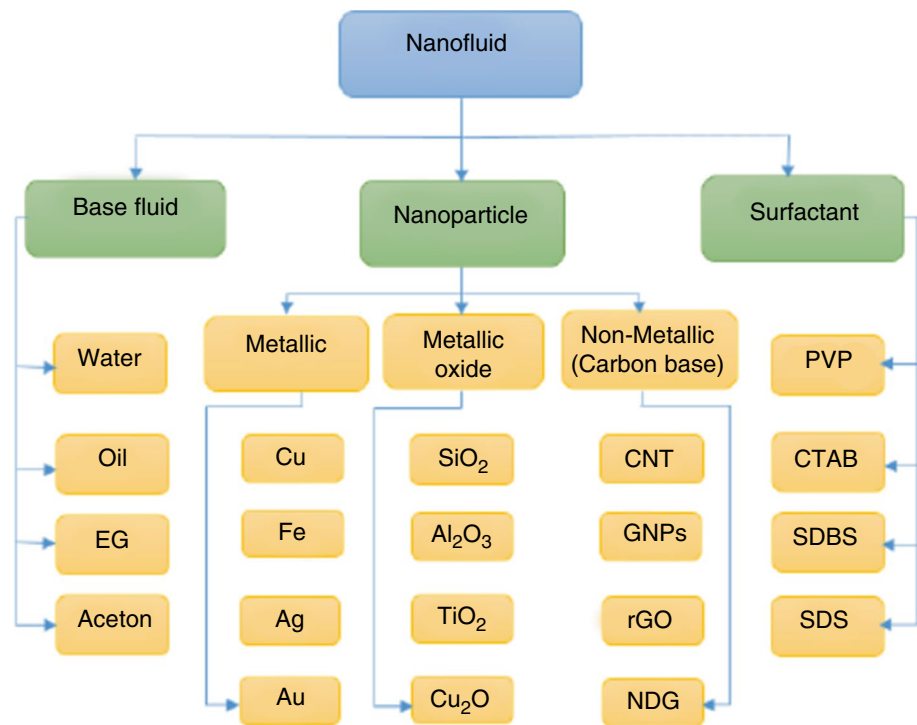
³ Institute of Advance Studies, University of Malaya, 50603 Kuala Lumpur, Malaysia

⁴ Department of Mechanical Engineering, College of Engineering, King Khalid University, PO Box 394, Abha 61421, Kingdom of Saudi Arabia

Introduction

Nanofluids are prepared by dispersing nanometer-scale sized solid particles in various base fluids like water, oil, ethylene glycol, etc., to enhance their thermal properties. Recent experimental investigations shown that the nanofluids exhibit substantially higher thermal conductivity compared to the base fluids [1]. The most common nanoparticles used for heat transfer enhancement were categorized as metal based, metal oxide based and carbon based like carbon nanotube, grapheme, etc., as shown in Fig. 1 [2]. The nanofluid is presented as next-generation heat transfer fluids; it has better thermal characteristics in comparison with the traditional heat transfer fluids. Over the past three decades, nanofluids displayed noteworthy development in thermal conductivity, heat transfer coefficients and stability which in turn reduce the overall power consumptions and cost of operation [3–7]. Nanofluids could be used in various heat exchangers to reduce overall energy consumption of industry. Thus, to identify a suitable suspension fluid with higher thermal conductivity and enhanced heat transfer

Fig. 1 Common base fluids, nanoparticles, and surfactants for nanofluids preparation



characteristics has become a challenge to the researchers and the potential users [8–13].

Several studies reported the improvement of thermal conductivity of heat transfer fluid depending on the size and shape of nanosized particles [14–17]. Moreover, the enhancement of thermal conductivity also depends on the addition and concentration of nanoparticles [18]. Besides the thermal behavior, the most crucial issue is the stability of the nanofluids and the achievement of the required stability is still an enormous challenge [19]. Several researchers had discussed about the stability of nanofluids; however, the results were inconclusive [20]. Some other researchers added different additives to the nanofluids to enhance their stability. The addition of Arabic gum, tragacanth gum, cetyltriethyl ammonium bromide (CTAB) and dodecyl benzene sulfate (SDBS) surfactants was tested where positive results were obtained, but the drawback is the pH of the fluids which were changed most of the time. The pH of suspension fluid has to be controlled by researchers to enhance the stability of nanofluids [21, 22]. The addition of surfactant is easy and low cost; this is a preferable method for industrial applications, but the fluidity and stability of the nanofluid cannot last long because of the loss of electrostatic repulsion when the distance between the nanoparticles becomes shorter [23]. Recently, it is found that minimizing the concentration of nanoparticle could be the best method to maintain better stability and fluidity. There are many applications in which nanofluids could be utilized, for instance closed conduit heat exchangers nanorefrigerant boiling heat transfer

inside flattened channels, heat storage component with nanoparticles and finned heat exchanger [24–26]. The ethylene glycol-based nanofluids exhibit higher thermal conductivity compared to the traditional working fluid. High thermal conductivity of cooling liquids (nanofluids) for microelectronic-mechanical systems could dissipate large amount of heat and solve their heat generation problems [27–29].

In recent years, the geometry of the heat exchanger conduit is becoming a great interest of study, both in numerically and experimentally [30–37]. Researchers around the globe used different geometry and flow configurations to investigate the thermal performance [38–41]. Therefore, it is a great interest to conduct research on the thermal performance and momentum transport of nanofluids in various configurations of flow passages and explore the possibilities of enhancement in heat transportation. Nanofluids have been receiving a substantial attention in the last 2 decades, for their improved thermal properties [42, 43]. The research shows that the heat transfer performance of nanofluids depends on many factors, for example effect of magnetic field, particle size, material and shape, fluid and temperature [44–47]. Al-Nimr et al. and Peyghambarzadeh et al. [48, 49] identified the features of nanofluids which are vital for numerous engineering applications. These special qualities include:

- Enhanced thermal conductivities.
- Increased ability of heat transfer.
- Justified pumping power.

- Supreme lubrication.
- Acceptable clogging and erosion within microchannels.

The concept of using suspension fluids has been driven by the prospective of improved heat exchanger fluids, where considerable enhancement of convection and thermal conduction properties is expected [50]. Many researchers conducted research on nanofluids for heat transfer applications [51–55]. Knowingly that the metal- and carbon-based materials in the solid form have thermal conductivities higher than the fluids [56–62]. The thermal conductivity of copper particles is approximately 700 times more than water at room temperature; therefore, the liquid that contains suspended copper particles should have significantly greater thermal conductivity than those of traditional heat transfer fluids [63]. Suspension fluids can be utilized in numerous engineering applications such as power plant cooling system, process industries, automobile, welding equipment industry and medical applications. Graphene nanofluids exhibit good heat capacity, improved stability when functionalized, excellent thermal conductivity and can be produced in mass quantities, and these are the main advantages over other nanomaterials. Moreover, depending on the production method, numerous physical properties and morphology of graphene can be obtained [64]. In that sense, the functionalized GNP is preferred over other nanomaterials.

In the wake of escalating global energy demand, the energy recovery by efficient means has become a vital issue. Heat exchangers are used for transportation and recovery of energy, so to develop efficient heat exchanger, the current work has emphasized on developing high-performance heat exchanger liquid and testing its performance in an experimental test rig. Heat transfer to nanofluids has been investigated for a long time by researchers and many of them concentrated on metal oxide with surfactant, but a few have adopted covalent functionalization for stability [65–69]. It has become essential to work on environmentally benign covalently functionalized synthesis of nanofluids for application in heat exchangers [70]. The present work has concentrated on the synthesis of carbon-based functionalized nanofluids and its application as heat exchanger liquid for the enhancement of heat transfer, save energy and provides economic benefits.

Material and methods

Graphene nanoplatelets (GNPs) of maximum particle width 2 μm , 99.5% purity and 750 $\text{m}^2 \text{g}^{-1}$ specific surface area were purchased from BT Science Sdn. Bhd. Analytical graded, hydrogen peroxide (30%) was procured from Sigma-Aldrich. Clove bud (CB) was procured from grocery stores at Kuala Lumpur, Malaysia.

The technique used for the preparation of GNP nanofluid is an environmental friendly one, which utilized dried clove buds in a polar solvent. This is a well-established technique, and it is suitable for investigation of various geometry conduits. This method also guaranteed the improvement of stability. In this technique, hydrogen peroxide was used to graft the main components of cloves (eugenol) onto GNPs. The hydrogen peroxide is considered as an oxidizer for producing a nontoxic substance. This functionalization technique can be separated into two phases, such as preparation of the clove extract and functionalization process. Figure 2 shows the procedure of preparation of GNP nanofluid which was started by adding 15 g of grounded clove buds into 1000 mL of distilled water at 80 °C; then, the solution was harmonized by a homogenizer at the speed of 1200 rpm. The solution was then heated continuously at 80 °C for 30 min. Then the solution was filtered by polytetrafluoroethylene (PTFE) 45- μm membrane in a vacuum filtration system.

The functionalization stage was performed systematically; for example, 5 g of pristine GNPs was added into a bowl containing 1000 mL of previously produced clove extract solution. In order to get a homogenous black solution, the suspension was agitated for 15 min continuously. The solution was then ultra-sonicated for 10 min, and during this mixing process, 25 mL of hydrogen peroxide was added drop by drop to the solution. The solution was then heated at 80 °C under reflux for 14 h. Then at 11,000–14,000 rpm, the produced fluid was centrifuged and washed by adding plenty of demineralized water until the pH of the fluid became neutral. After that, the functionalized sample was dried for 12 h in a vacuum oven at 60 °C. Then, the CGNP–water nanofluids were synthesized by adding calculated amount of CGNP powder to the distilled water and then sonicated for 10 min to disperse CGNPs into distilled water. In the present investigation, the particle concentrations were maintained at 0.1, 0.075 and 0.025 mass%. The clove-treated GNPs were found extremely stable in the aqueous medium.

Experimental

In the field of thermo-fluid, the performance of a heat exchanger test rig can be improved by enhancing its heat transfer coefficient (h).

The experimental setup used in this investigation is shown in Fig. 3 which consists of four main sections, heating unit, flow loop, cooler, measuring tools and the control unit. The flow loop contains pump, pressure gage, transmitter of differential pressure, cooler, thermocouples, flow meter, power supply and the test section.

Figure 4 shows the schematic diagram and the photograph of the test section. The experimental investigation was conducted in two stainless steel horizontal straight tubes of rectangular and circular cross sections with the inner diameter

Fig. 2 Steps of preparing functionalized GNP with clove bud extract

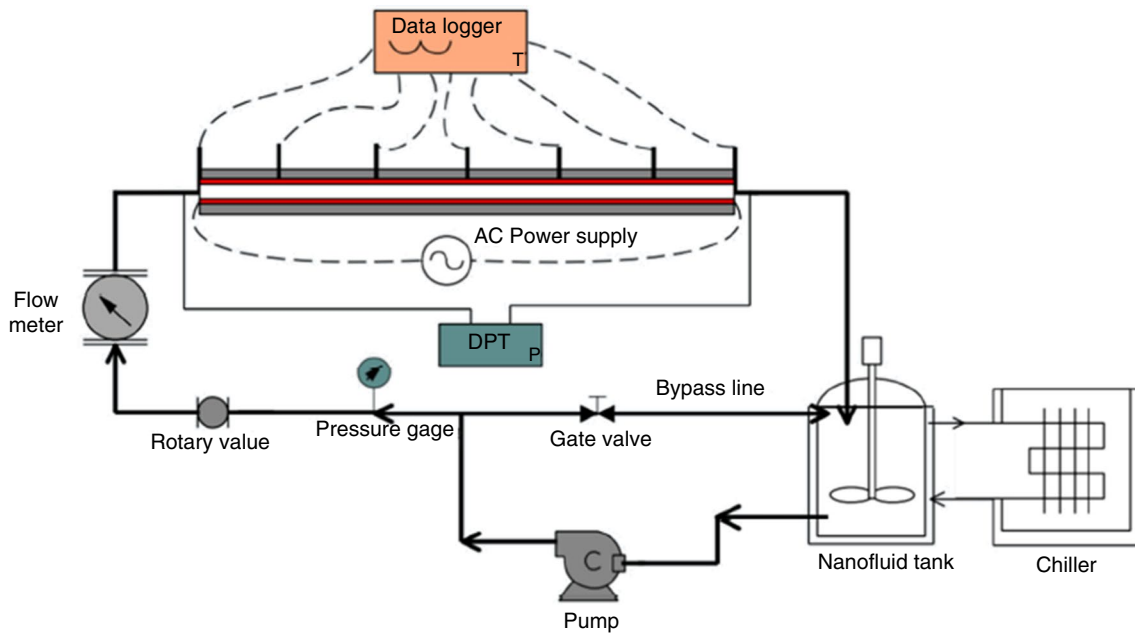
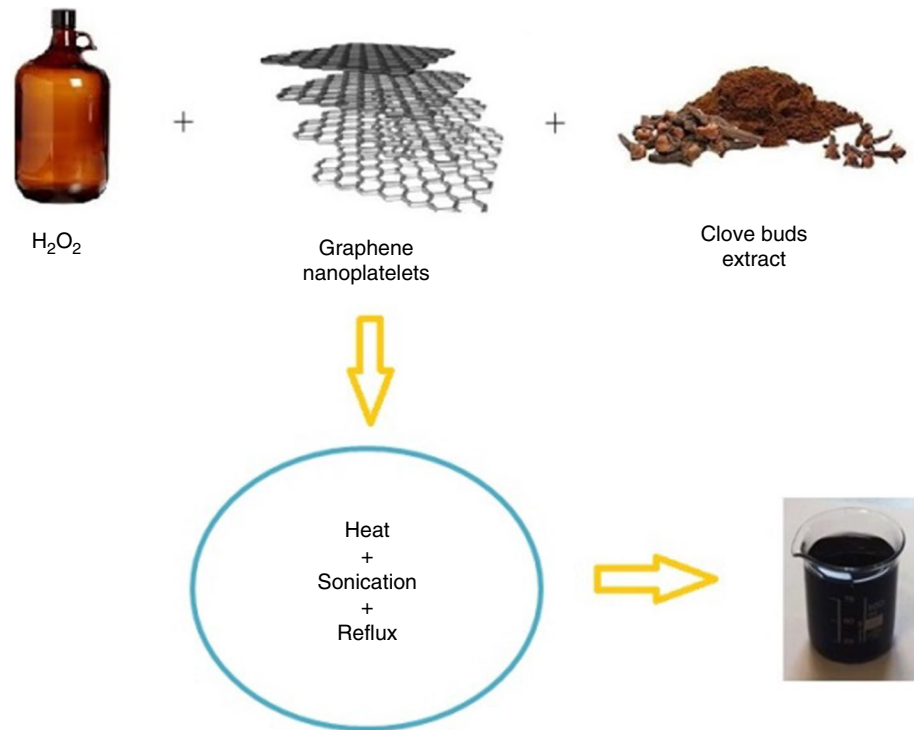


Fig. 3 Experimental setup for investigation of the convection heat transfer coefficient

of 10 mm and the length 1400 mm. The heated portion of the tube was installed by carefully wrapping the outer surface of the test section up to the length of 1200 mm. The test section was wrapped by an electrical heating element which regulated by a transformer of variable voltage output. The maximum power capacity of the heating element was

900 W. It is known that the heated fluid dissipates a portion of the heat to the surroundings by radiation and convection. Heat was transferred from the heated surface to the cold fluid flowing through the test section. Outer surface of the heater tape and the tubes were wrapped properly by a thick layer of insulation glass wool (50 mm) throughout the length of the

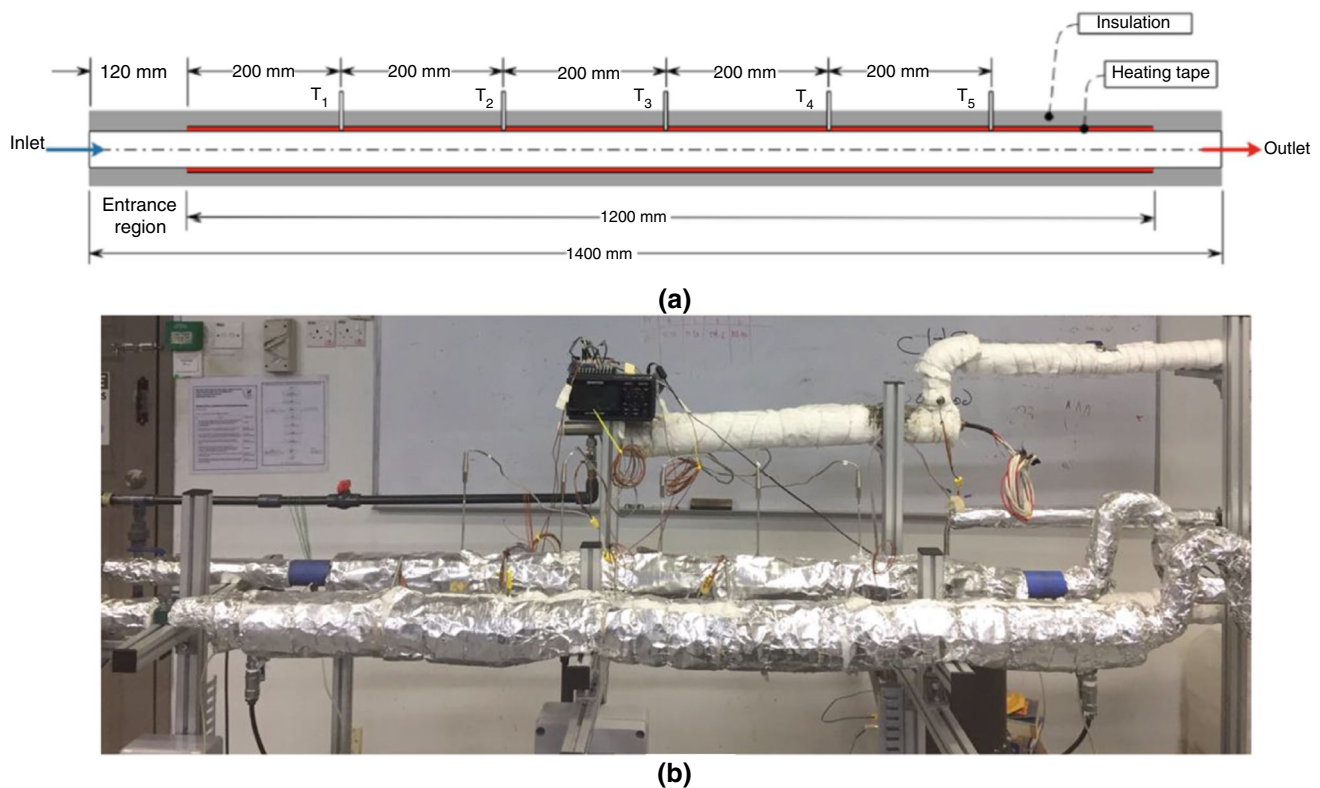


Fig. 4 Sectional view of the experimental test section. **a** Schematic diagram. **b** Actual test section

tubes, and finally, the outer surface of the insulation layers was covered by aluminium foil to minimize radiation and natural convection heat losses to the surroundings.

To estimate the heat transfer to the flowing fluids from the tape-heated tube test section, five equally spaced K-type thermocouples of (± 0.1 °C) accuracy were fixed by using high thermal conductive epoxy adhesive material to measure the surface temperatures. The bulk temperature and the inlet and outlet temperatures of the fluid were measured by two thermal sensors (PT 100).

In the flow loop of the experimental setup, the fluid was pumped by EX-70R magnetic pump of capacity 80 L min^{-1} , from a reservoir of capacity 10 L covered with a cooling jacket to keep a uniform temperature of the fluid in the reservoir. The fluid in the reservoir was kept under constant stirring to prevent sedimentation of the particles inside the tank. After completion of a cycle in the flow loop, the fluid was returned back to the jacketed tank where the hot fluid was cooled by the chiller which regulated the flow of chilled water to the reservoir jacket to remove the heat from the main stream fluid. In the flow passage, the pressure drop across the test section was measured by using a pressure transducer of OMEGA with an accuracy of $\pm 0.75\%$. All the temperatures were recorded in a Graphtec GL-800 multichannel electronic data logger, and the pressure drop, flow

rate and heat flux data were noted and compiled in a computer for data processing.

Properties of nanofluids

Dispersion of nanoparticles in a host fluid alters the thermophysical properties of the suspension fluid. Many researchers have tried to improve the thermophysical properties of the conventional heat exchanging liquids by dispersing nanoparticles in the base fluids. Improvement of the synthesized nanofluid properties was theoretically evaluated by many researchers from the various correlations developed for suspension fluids. The experimental data of any dispersed nanofluid could be compared with the evaluated characteristics of the nanofluids from the correlations for validation of data and to explore the reason of positive enhancement in properties.

Nanofluids were explored by the investigators to obtain the improvement of thermal conductivity of the fluid for application in heat exchangers. Many experiments were conducted to compare the experimental results with the analytical solutions. One of those models was presented by Crosser and Hamilton who investigated the effects of the ratios of surface areas of spheres with the volumes of the nanoparticles on thermal conductivity of nanofluids, as shown in Eq. (1) [71].

$$K_{nf} = K_{bf} \left[\frac{K_p + (n - 1)K_{bf} - (n - 1)\beta_p (K_{bf} - K_p)}{K_p + (n - 1)K_{bf} - \beta_p (K_{bf} - K_p)} \right] \quad (1)$$

where K_{nf} is the thermal conductivity of nanofluid, K_p is the thermal conductivity of the nanoparticles, K_{bf} is the thermal conductivity of the base fluid and β is the ratio of the nanolayer thickness to the original particle radius. Generally, the value of $\beta=0.1$ is selected in the calculation of the thermal conductivity of nanofluids, $n = \frac{3}{\phi}$ which is the experimental shape factor in Eq. (1) and ϕ is representing the sphericity of the nanoparticles as mentioned above. Thermos-physical characteristics of nanofluid are essentially relied on the properties of the host fluids, such as pH, size and volume concentration values of the solid nanoparticles.

Considering balance mass of the mixture of host fluid and solid nanoparticles, the effective density (ρ_{nf}) of nanofluid can be calculated by Eq. (2).

$$\rho_{nf} = (1 - \phi_p)\rho_{bf} + \phi_p \rho_p \quad (2)$$

where ρ_{bf} , ρ_p , and ϕ_p are the density of the host fluid, the density of particles and the volume fraction of the solid nanoparticles, respectively.

Xuan and Roetzel [72] improved a formula to obtain the specific heat of suspended fluid as shown in Eq. (3).

$$C_{p,nf} = \frac{(1 - \phi_p)\rho_{bf} C_{bf} + \phi_p \rho_p C_p}{\rho_{nf}} \quad (3)$$

Viscosity is one of the most important properties of the nanofluids, and the results of pressure drop, pumping power and heat transfer are relying on it. Sharma et al. [73] tried to find a correlation for this property taking into account the particle diameter, volume portion and temperature as shown in Eq. (4).

$$\mu_{nf} = \left[(1 + \phi_p)^{11.3} \left(1 + \frac{T_{nf}}{70} \right)^{-0.038} \left(1 + \frac{d_p}{170} \right)^{-0.061} \right] \mu_{bf} \quad (4)$$

Table 1 shows the thermophysical properties of the tested materials. The presented correlations were used to calculate the most important thermophysical properties of the

nanofluids. Those properties are the density, specific heat, thermal conductivity and viscosity.

Data reduction for evaluation of heat transfer and pressure drop

Calculation of pressure drop between the inlet and outlet of the test section when the fluid flows through the tube considered one of the most important characteristics of the nanofluids for specifying the power requirement for the pump as it depends on the pressure drop through the tube.

To evaluate the drop of pressure through the tubes, calculation of Darcy friction factor (C_f) is essential by using Eq. (5).

$$C_f = \frac{\tau_s}{\frac{\rho V^2}{2}} \quad (5)$$

where τ_s indicates the shear stress and the average velocity is denoted by V .

Fanning friction coefficient f can be correlated with Darcy friction factor as shown in another Eq. (6).

$$C_f = \frac{f}{4} \quad (6)$$

Friction factor property should be evaluated to calculate the pressure drop in the ducts, and this feature depends mainly on flow regime and Reynolds number. When the fluid flows through the ducts in the laminar regime, then the friction factor can be calculated based on Eq. (7).

$$f = \frac{64}{Re} \quad (7)$$

Experiments of the current investigation were performed in the turbulent flow regime, where the friction factors were calculated from the empirical equations or from the Moody chart where the surface roughness property was obtained from the tables [74]. The pressure drop can be evaluated theoretically by Eq. (8).

$$\Delta P = f \left(\frac{L}{D} \right) \frac{\rho V^2}{2} \quad (8)$$

In the case of testing different nanofluids, if the Reynolds number is kept constant, then the velocity of the different nanofluids at different concentrations could be changed, as

Table 1 Thermophysical properties of the nanofluids

| Nanofluid | $\mu/\text{Pa s}$ | $P/\text{m}^3 \text{kg}^{-1}$ | $C_p/\text{J kg}^{-1} \text{K}^{-1}$ | $k/\text{W m}^{-1} \text{K}^{-1}$ | Pr |
|-----------|-------------------|-------------------------------|--------------------------------------|-----------------------------------|----------|
| DW | 8.29E-04 | 995.5 | 4142 | 0.611 | 5.62E+00 |
| GNP0.025 | 0.000844 | 995.6 | 4123 | 0.636 | 5.47E+00 |
| GNP0.075 | 0.000868 | 995.8 | 4096 | 0.681 | 5.22E+00 |
| GNP0.1 | 0.000885 | 995.9 | 4080 | 0.708 | 5.10E+00 |

the viscosity and density alter the relation between Re and V, as shown in Eq. (9).

$$V = \frac{Re\mu}{\rho D} \tag{9}$$

By substituting the velocity from Eq. (9) in Eq. (8), then the drop of pressure per unit length can be calculated by the resulting Eq. (10).

$$\frac{\Delta P}{L} = \frac{Re^2 f}{2D^3} v \cdot \mu \tag{10}$$

In the case of turbulent flow, friction factor can be determined by employing Petukhov Eq. (11).

$$Nu_{nf} = f \left[Re, Pr, \frac{K_p (\rho C_p)_p}{K_{bf} (\rho C_p)_{bf}}, \emptyset, \text{ flow geometry, particle geometry} \right] \tag{16}$$

$$f = (0.79 \ln Re - 1.64)^{-2} \tag{11}$$

Regarding the calculations of heat flux, heat transfer coefficient and Nusselt number of the flowing fluids through the ducts are discussed by many researchers and most of the correlations generated are dependent on which type of flow regime, flow passage configuration, type of fluid and properties of the fluid. Gnielinski [75] presented a correlation for evaluating Nusselt number in the fully developed flow in circular tube at various boundary conditions, as shown in Eq. (12).

$$Nu = \frac{\left(\frac{f}{8}\right)(Re - 1000) Pr}{1 + 12.7\sqrt{\frac{f}{8}}(Pr^{2/3} - 1)} \left[1 + \left(\frac{D}{L}\right)^{2/3} \right] k_c \tag{12}$$

where k_c is consider as a factor which can be obtained from the Prandtl number ratio of the fluids as presented by Eq. (13).

$$k_c = \left(\frac{Pr}{Pr_s}\right)^{0.11} \tag{13}$$

Here, Pr_s is referring to the Prandtl number at the surface temperature, whereas Pr can be calculated by Eq. (14), considering bulk temperature of the fluid.

$$Pr = \frac{\mu C_p}{K} \tag{14}$$

Dittus and Boelter developed an experimental correlation to evaluate Nusselt number at fully developed flow through the tubes as presented by Eq. (15).

$$Nu = 0.023 Re^{0.8} Pr^n \tag{15}$$

When the fluid is heated, then $n = 0.4$; whereas, $n = 0.3$ if the fluid is cooled.

With reference to Eqs. (12 and 15), the Reynolds number and Prandtl number can be considered as the two parameters affecting the value of Nusselt number in the case of forced convection turbulent flow heat transfer. So, the enhancement effect will come from the Prandtl number in the case of keeping Reynolds number constant.

Xuan and Roetzel [72] investigated the Nusselt number and examined the parameters which could affect Nu, and later they suggested a new general function containing the influence factors of Nusselt number as presented by Eq. (16).

From the Newton’s law for cooling as shown in Eq. (1), the average value of heat transfer coefficient for convection can be calculated from Eq. (17).

$$h = \frac{NuK}{D} = \frac{q}{(T_s - T_b)} \tag{17}$$

where q represents the heat flux, T_s represents the temperature of the inner surface and T_b represents the bulk temperature of the flowing fluid. This equation can also be used to evaluate the local Nusselt number at a specific location in the test section based on the temperature of the fluid and the surface temperature recoded at the specific location of the surface.

Thermophysical properties of the fluid needs to be considered after adding nanoparticles in the base fluid to evaluate the corresponding velocity of the nanofluid considering based fluid velocity. So, Eq. (18) can be used to calculate the velocity of nanofluid at constant Reynolds number.

$$V_{nf} = \frac{\rho_{bf} \mu_{nf}}{\rho_{nf} \mu_{bf}} V_{bf} \tag{18}$$

where V_{bf} represents the base fluid velocity and could be calculated from Eq. (9), considering fluid bulk temperature.

Results and discussions

Validations of the data from the test rig

The experimental test rig with both the circular and square test sections was first validated by comparing the data of Nusselt number obtained experimentally with those obtained by the empirical correlations (Dittus–Boelter and

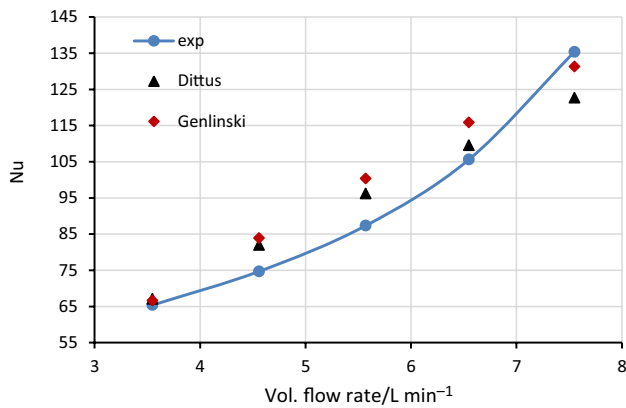


Fig. 5 Profile of Nusselt number for circular test section

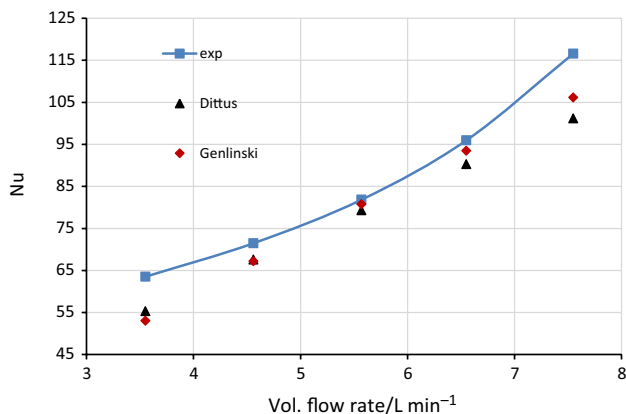


Fig. 6 Profile of Nusselt number for square test section

Gnielinski). Figure 5 shows a good agreement between the experimental data of Nusselt number for the circular test section and those obtained for the circular tube from empirical correlations of Gnielinski and Dittus–Boelter with the average errors of 9.05% and 7.98%, respectively. Experimental data satisfied the data obtained from standard equations within the limited percentage of variations.

Figure 6 illustrates the difference between the average Nusselt numbers calculated by the empirical correlations for the square test section. The average errors between the Nusselt numbers obtained experimentally and from standard correlations of Dittus and Gnielinski are 6.9% and 7.5%, respectively.

The average errors for both the circular and square test sections are less than 10% which indicates that the data generated from the test rig are satisfactory and can be utilized to evaluate the convection heat transfer coefficients of different fluids to compare with the data obtained for water alone. Another method to evaluate the reliability and accuracy of the experimental system can be done by comparing the

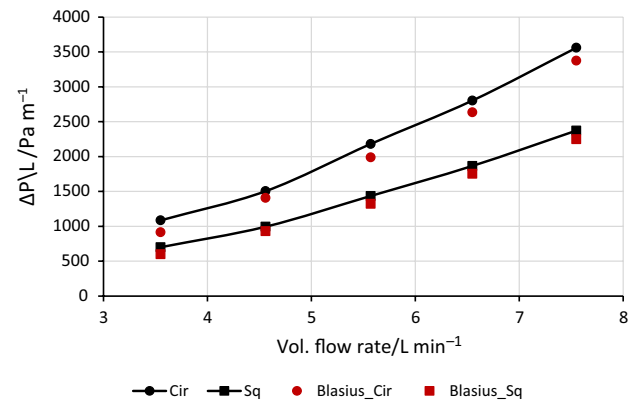


Fig. 7 Profile of measured pressure drops for the circular and square test sections comparing with the calculated pressure drops using Blasius equation

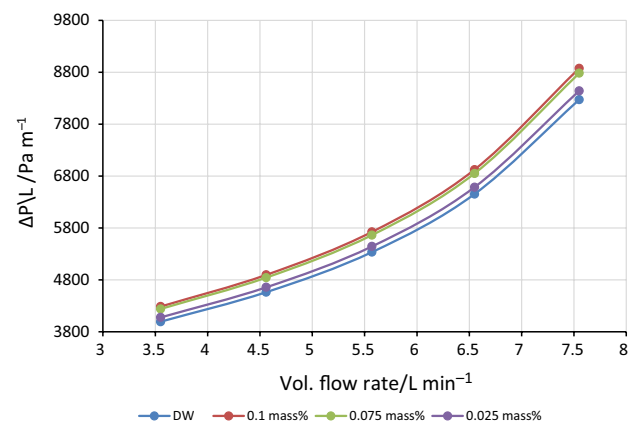


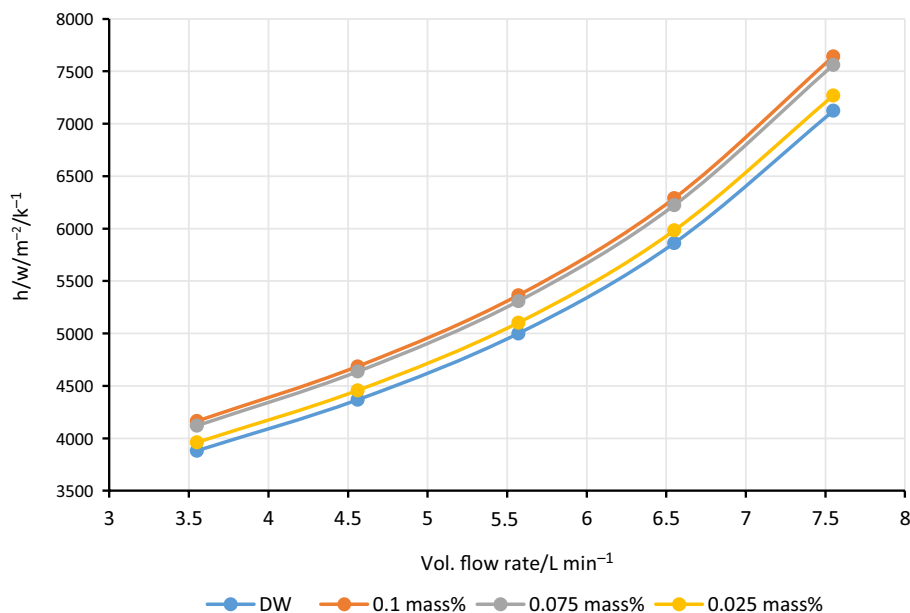
Fig. 8 Average values of heat transfer coefficients at various volume flow rates for the circular test section

pressure drop measured experimentally and those obtained by the empirical equation such as the Blasius' equation for both the circular and square test sections at the same range of volume flow rates. Figure 7 shows a good agreement between the measured pressure drops per unit length of the tube with the calculated data by Blasius equation for both the circular and square test sections with the evaluated average errors of 9.4% and 8.8%, respectively. The results indicate satisfactory accuracy level of the current investigations of the pressure drop measurements.

Heat transfer of nanofluids

These experiments were conducted with distilled water and GNP nanofluids of three different concentrations such as 0.025 mass%, 0.075 mass% and 0.1 mass% of nanoparticles in turbulent forced flow condition. Evaluation of heat transfer performance was obtained by examining the

Fig. 9 Average values of heat transfer coefficients at various volumetric mass flow rates for the square test section



parameters like heat transfer coefficient and Nusselt number. These parameters were calculated by considering the average values in the fully developed region. Figures 8 and 9 show that, with the increase in the volume flow rate, the heat transfer coefficient was increased. The graphs show a noticeable increase in the value of heat transfer coefficient with the growing concentrations of nanoparticles in both the test sections, the circular and square. This can be attributed to the Brownian motion of the nanoparticles which enhanced advection and augmented heat transfer coefficient consequently. The average ratios of enhancement in heat transfer coefficients are 2.05%, 6.15% and 7.29% for 0.025 mass%, 0.075 mass% and 0.1 mass% concentrations, respectively, for both the test sections.

Another important point to be explained is that the rate of heat transfer in the square test section is less than the circular test section, although in the square section the secondary flow and swirls formation occurs at the corners which in turn could enhance the rate of heat transfer, but in this case the cross section of the square test section is higher than the circular test section, which reduced the velocity and Reynolds number for the same flow rate the reduction in the Nusselt number and heat transfer coefficient.

Regarding Nusselt number, it is primarily dependent on two types of non-dimensional numbers which are Reynolds and Prandtl numbers. The experiment showed that by increasing the concentrations of nanoparticles, noticeable reductions in the values of Prandtl number were observed, and the Reynolds number was decreased as well due to the increasing kinematic viscosity and density at the same flow velocity.

Decreasing Prandtl number (the ratio of momentum diffusivity to thermal diffusivity) is a notable reason for the reduction in the Nusselt number; even though the dynamic viscosity is increased, which is proportional to Prandtl number, Prandtl number is declined due to the increase in the thermal conductivity by raising the concentration of nanoparticles, which is inversely proportional to Prandtl number, and it has higher average growth than dynamic viscosity which leads to decreasing Prandtl number. As a result, Nusselt number is decreased because of the reduction in the values of Reynolds and Prandtl number. Figures 10 and 11 show the reduction in Nusselt number for both the test sections.

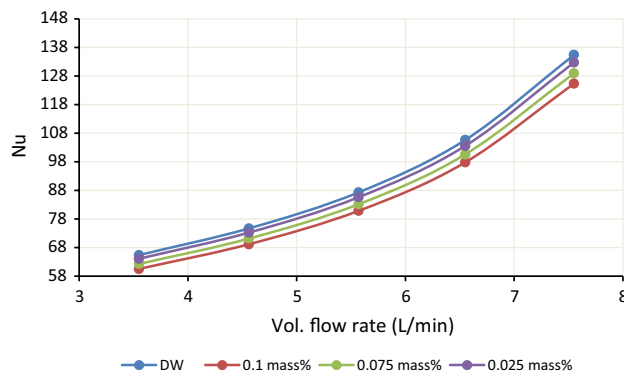


Fig. 10 Variations of Nusselt number with the volumetric mass flow rates for the circular test section

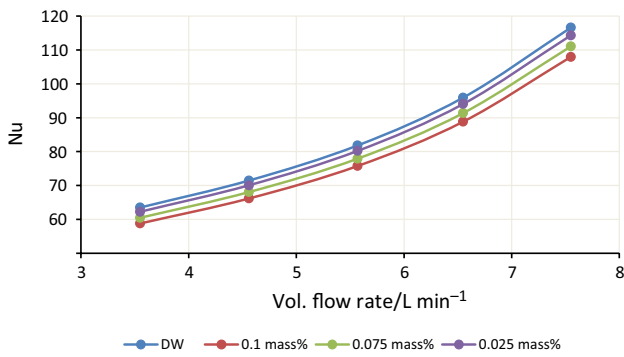


Fig. 11 Variations of Nusselt number with the volumetric mass flow rates for the square test section

Pressure drop of nanofluid

Researchers investigated the pressure drop across the test section of the closed conduit flow under intensive investigations, which is the most important parameter to evaluate the requirements of pump and fan power, following the importance of energy conservation in industrial field.

The pressure drop mainly depends on friction factor which also depends on the flow regime and roughness of the tube. In the present investigation, the flow was turbulent; hence, the friction factor was calculated from Eq. (11); then, the pressure drop per unit length was determined by applying Eq. (10).

Figures 12 and 13 show the increase in the concentration of nanoparticles enhancing the pressure drop. This observation confirms the significance of GNP concentration on the viscosity of nanofluid. The average ratios of increase in the

Fig. 12 Pressure drop profile per unit length for various volumetric mass flow rates through the circular test section

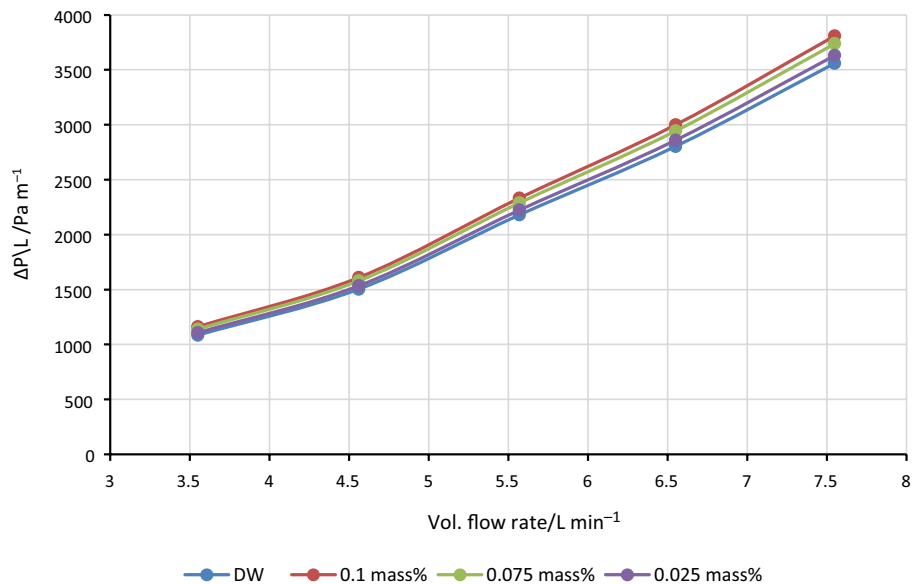
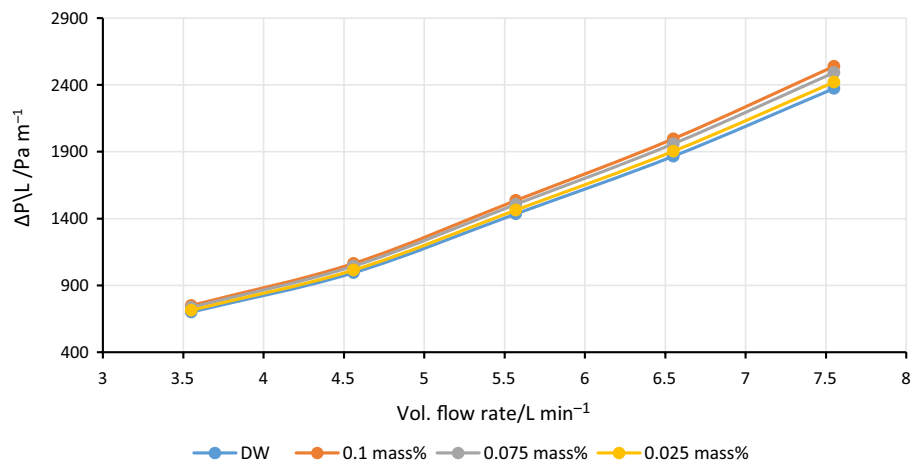


Fig. 13 Pressure drop profile per unit length for various volumetric mass flow rates through the square test section



pressure drop with the rise of concentrations are 2%, 5% and 7% for 0.025 mass%, 0.075 mass% and 0.1 mass%, respectively, for circular and square test sections.

For a certain volumetric flow rate, the graphs show that the pressure drop along the square test section is less than that of the circular tube test section. For example at 0.1 mass% of GNP concentration, the pressure drop is around 35% less compared to water data in the square test section. This observation can be attributed to the increase in hydraulic diameter in the square test section which provides a proportional relation with the generated pressure drop. Equation (10) further validates the inference.

Conclusions

In this study, GNP was functionalized covalently by clove buds extract and dispersed in water for synthesizing CGNPs nanofluids at various particle concentrations such as 0.025, 0.075 and 0.1 mass%. The prepared nanofluids were tested in horizontal circular and square pipe heat exchanger where the heat transfer and frictional pressure loss data were evaluated. The present investigation highlighted several new insights towards pursuing an enhancement in convective heat transfer by the alteration of flow passage and evaluation of the pressure drop in different configurations of the heat exchanger tubes. From the investigation, the following conclusions were drawn:

- GNP nanofluid coolant enhances the heat transfer coefficient irrespective of the flow passage configurations (circular and square).
- Heat transfer coefficient significantly increased with the increase in concentration of GNP in the coolant.
- Nusselt number decreases with the increase in the concentrations of GNP, and the decrease in the Prandtl number is accompanied by increasing the concentrations of nanoparticles.
- There is a considerable enhancement of frictional pressure drop with the increase in the concentration of GNP nanoparticles in the fluid.
- The Nusselt number in the circular test section is higher than that obtained in the square test section, because the increase in the hydraulic diameter in the square test section for a certain volumetric mass flow rate leads to decrease in the velocity, Reynolds number and the rate of heat transfer.
- In the future, experimental investigation at constant surface temperature approach could be done and compared with the data at constant heat flux boundary condition.

Acknowledgements The authors acknowledge the contribution of Research Grants IF056-2019, FP143-2019A and King Khalid University Grant, G.R.P-119- 41.

References

1. Eastman J, Choi U, Li S, Thompson L, Lee S. Enhanced thermal conductivity through the development of nanofluids. In: MRS Proceedings vol 457. Cambridge University Press; 2016.
2. Solangi KH, Luhur MR, Badarudin A, Amiri A, Rad Sadri, Zubir MNM, Samira Gharehkhani, Teng KH. A comprehensive review of thermo-physical properties and convective heat transfer to nanofluids. *Energy*. 2015;89:1065–86.
3. Ramezanizadeh M, Ahmadi MA, Ahmadi MH, Alhuyi Nazari M. Rigorous smart model for predicting dynamic viscosity of Al₂O₃/water nanofluid. *J Therm Anal Calorim*. 2019;137(1):307–16.
4. Maddah H, Aghayari R, Ahmadi MH, Rahimzadeh M, Ghasemi N. Prediction and modeling of MWCNT/Carbon (60/40)/SAE 10 W 40/SAE 85 W 90(50/50) nanofluid viscosity using artificial neural network (ANN) and self-organizing map (SOM). *J Therm Anal Calorim*. 2018;134(3):2275–86.
5. Ahmadi MH, Ahmadi MA, Nazari MA, Mahian O, Ghasempour R. A proposed model to predict thermal conductivity ratio of Al₂O₃/EG nanofluid by applying least squares support vector machine (LSSVM) and genetic algorithm as a connectionist approach. *J Therm Anal Calorim*. 2019;135(1):271–81.
6. Ahmadi MH, Alhuyi Nazari M, Ghasempour R, Madah H, Shafii MB, Ahmadi MA. Thermal conductivity ratio prediction of Al₂O₃/water nanofluid by applying connectionist methods. *Colloids Surf A Physicochem Eng Asp*. 2018;541:154–64.
7. Maddah H, Aghayari R, Mirzaee M, Ahmadi MH, Sadeghzadeh M, Chamkha AJ. Factorial experimental design for the thermal performance of a double pipe heat exchanger using Al₂O₃-TiO₂ hybrid nanofluid. *Int Commun Heat Mass Transfer*. 2018;97:92–102.
8. Chen H, Witharana S, Jin Y, Kim C, Ding Y. Predicting thermal conductivity of liquid suspensions of nanoparticles (nanofluids) based on rheology. *Particuology*. 2009;7(2):151–7.
9. Baghban A, Pourfayaz F, Ahmadi MH, Kasaeian A, Pourkiaei SM, Lorenzini G. Connectionist intelligent model estimates of convective heat transfer coefficient of nanofluids in circular cross-sectional channels. *J Therm Anal Calorim*. 2018;132(2):1213–39.
10. Mohseni-Gharyehsafa B, Ebrahimi-Moghadam A, Okati V, Farzaneh-Gord M, Ahmadi MH, Lorenzini G. Optimizing flow properties of the different nanofluids inside a circular tube by using entropy generation minimization approach. *J Therm Anal Calorim*. 2019;135(1):801–11.
11. Ahmadi MA, Ahmadi MH, Fahim Alavi M, Nazemzadegan MR, Ghasempour R, Shamsirband S. Determination of thermal conductivity ratio of CuO/ethylene glycol nanofluid by connectionist approach. *Journal of the Taiwan Institute of Chemical Engineers*. 2018;91:383–95.
12. Baghban A, Jalali A, Shafiee M, Ahmadi MH, Chau KW. Developing an ANFIS-based swarm concept model for estimating the relative viscosity of nanofluids. *Engineering Applications of Computational Fluid Mechanics*. 2019;13(1):26–39.
13. Ahmadi MH, Mirlohi A, Alhuyi Nazari M, Ghasempour R. A review of thermal conductivity of various nanofluids. *J Mol Liq*. 2018;265:181–8.
14. Sheikholeslami M, Shehzad SA. CVFEM for influence of external magnetic source on Fe₃O₄-H₂O nanofluid behavior in a permeable cavity considering shape effect. *Int J Heat Mass Transf*. 2017;115:180–91.

15. Sheikholeslami M, Shehzad SA. Numerical analysis of Fe₃O₄-H₂O nanofluid flow in permeable media under the effect of external magnetic source. *Int J Heat Mass Transf.* 2018;118:182–92.
16. Sheikholeslami M, Rokni HB. Numerical simulation for impact of Coulomb force on nanofluid heat transfer in a porous enclosure in presence of thermal radiation. *Int J Heat Mass Transf.* 2018;118:823–31.
17. Babazadeh H, Zeeshan A, Jacob K, Hajizadeh A, Bhatti MM. Numerical modelling for nanoparticle thermal migration with effects of shape of particles and magnetic field inside a porous enclosure. *Iran J Sci Technol Trans Mech Eng.* 2020. <https://doi.org/10.1007/s40997-020-00354-9>.
18. Halelfadl S, Estellé P, Maré T. Heat transfer properties of aqueous carbon nanotubes nanofluids in coaxial heat exchanger under laminar regime. *Exp Thermal Fluid Sci.* 2014;55:174–80.
19. Noroozi M, Radiman S, Zakaria A. Influence of Sonication on the Stability and Thermal Properties of Al₂O₃ Nanofluids. *Journal of Nanomaterials.* 2014;2014:10.
20. Teng TP, Fang YB, Hsu YC, Lin L. Evaluating Stability of Aqueous Multiwalled Carbon Nanotube Nanofluids by Using Different Stabilizers. *Journal of Nanomaterials.* 2014;2014:15.
21. Barber J, Brutin D, Tadrist L. A review on boiling heat transfer enhancement with nanofluids. *Nanoscale Res Lett.* 2011;6(1):280.
22. Nkurikiyimfura I, Wang Y, Pan Z. Heat transfer enhancement by magnetic nanofluids-A review. *Renew Sustain Energy Rev.* 2013;21:548–61.
23. Harikrishnan S, Magesh S, Kalaiselvam S. Preparation and thermal energy storage behaviour of stearic acid-TiO₂ nanofluids as a phase change material for solar heating systems. *Thermochim Acta.* 2013;565:137–45.
24. Sheikholeslami M, Rezaeianjouybari B, Darzi M, Shafee A, Li Z, Nguyen TK. Application of nano-refrigerant for boiling heat transfer enhancement employing an experimental study. *Int J Heat Mass Transf.* 2019;141:974–80.
25. Sheikholeslami M, Haq RU, Shafee A, Li Z, Elaraki YG, Tlili I. Heat transfer simulation of heat storage unit with nanoparticles and fins through a heat exchanger. *Int J Heat Mass Transf.* 2019;135:470–8.
26. Nguyen-Thoi T, Bhatti MM, Ali JA, Hamad SM, Sheikholeslami M, Shafee A, et al. Analysis on the heat storage unit through a Y-shaped fin for solidification of NEPCM. *J Mol Liq.* 2019;292:111378.
27. Saidur R, Leong KY, Mohammad HA. A review on applications and challenges of nanofluids. *Renew Sustain Energy Rev.* 2011;15(3):1646–68.
28. Nguyen T, Mochizuki M, Mashiko K, Saito Y, Sanciuc I, Boggs R. Advanced cooling system using miniature heat pipes in mobile PC. *IEEE Trans Compon Packag Technol.* 2000;23(1):86–90.
29. Matsuda M, Mochizuki M, Saito Y, Mashiko K, Nguyen T. Two phase closed loop cooling system with a pump. In: 15th IEEE intersociety conference on thermal and thermomechanical phenomena in electronic systems (ITherm) 31 May–3 June; 2016.
30. Sheikholeslami M. New computational approach for exergy and entropy analysis of nanofluid under the impact of Lorentz force through a porous media. *Comput Methods Appl Mech Eng.* 2019;344:319–33.
31. Manh TD, Nam ND, Abdulrahman GK, Moradi R, Babazadeh H. Impact of MHD on hybrid nanomaterial free convective flow within a permeable region. *J Therm Anal Calorim.* 2019. <https://doi.org/10.1007/s10973-019-09008-8>.
32. Sheikholeslami M, Shehzad SA. CVFEM simulation for nanofluid migration in a porous medium using Darcy model. *Int J Heat Mass Transf.* 2018;122:1264–71.
33. Sheikholeslami M, Ghasemi A, Li Z, Shafee A, Saleem S. Influence of CuO nanoparticles on heat transfer behavior of PCM in solidification process considering radiative source term. *Int J Heat Mass Transf.* 2018;126:1252–64.
34. Sheikholeslami M, Li Z, Shafee A. Lorentz forces effect on NEPCM heat transfer during solidification in a porous energy storage system. *Int J Heat Mass Transf.* 2018;127:665–74.
35. Sheikholeslami M, Shehzad SA, Li Z, Shafee A. Numerical modeling for alumina nanofluid magnetohydrodynamic convective heat transfer in a permeable medium using Darcy law. *Int J Heat Mass Transf.* 2018;127:614–22.
36. Alawi OA, Sidik NAC, Kazi SN, Najafi G. Graphene nanoplatelets and few-layer graphene studies in thermo-physical properties and particle characterization. *J Therm Anal Calorim.* 2019;135(2):1081–93.
37. Akram N, Sadri R, Kazi SN, Zubir MNM, Ridha M, Ahmed W, et al. A comprehensive review on nanofluid operated solar flat plate collectors. *J Therm Anal Calorim.* 2020;139(2):1309–43.
38. Mehryan SAM, Izadpanahi E, Ghalambaz M, Chamkha AJ. Mixed convection flow caused by an oscillating cylinder in a square cavity filled with Cu-Al₂O₃/water hybrid nanofluid. *J Therm Anal Calorim.* 2019;137(3):965–82.
39. Benzema M, Benkahla YK, Labsi N, Ouyahia S-E, El Ganaoui M. Second law analysis of MHD mixed convection heat transfer in a vented irregular cavity filled with Ag-MgO/water hybrid nanofluid. *J Therm Anal Calorim.* 2019;137(3):1113–32.
40. Nazari MA, Ghasempour R, Ahmadi MH, Heydarian G, Shafii MB. Experimental investigation of graphene oxide nanofluid on heat transfer enhancement of pulsating heat pipe. *Int Commun Heat Mass Transfer.* 2018;91:90–4.
41. Sheikholeslami M, Jafaryar M, Saleem S, Li Z, Shafee A, Jiang Y. Nanofluid heat transfer augmentation and exergy loss inside a pipe equipped with innovative turbulators. *Int J Heat Mass Transf.* 2018;126:156–63.
42. Li Z, Sheikholeslami M, Bhatti MM. Effect of Lorentz forces on nanofluid flow inside a porous enclosure with a moving wall using various shapes of CuO nanoparticles. *Heat Transfer Research.* 2019;50(7):697–715.
43. Sheikholeslami M, Bhatti MM. Influence of external magnetic source on nanofluid treatment in a porous cavity. *Journal of Porous Media.* 2019;22(12):1475–91.
44. Sheikholeslami M, Hayat T, Alsaedi A. On simulation of nanofluid radiation and natural convection in an enclosure with elliptical cylinders. *Int J Heat Mass Transf.* 2017;115:981–91.
45. Manh TD, Nam ND, Abdulrahman GK, Shafee A, Shamlooei M, Babazadeh H, et al. Effect of radiative source term on the behavior of nanomaterial with considering Lorentz forces. *J Therm Anal Calorim.* 2019. <https://doi.org/10.1007/s10973-019-09077-9>.
46. Sheikholeslami M, Sadoughi MK. Simulation of CuO-water nanofluid heat transfer enhancement in presence of melting surface. *Int J Heat Mass Transf.* 2018;116:909–19.
47. Sheikholeslami M, Rokni HB. Simulation of nanofluid heat transfer in presence of magnetic field: A review. *Int J Heat Mass Transf.* 2017;115:1203–33.
48. Al-Nimr MdA, Al-Dafaie AMA (2014) Using nanofluids in enhancing the performance of a novel two-layer solar pond. *Energy.* 2014;68:318–26.
49. Peyghambarzadeh SM, Hashemabadi SH, Chabi AR, Salimi M. Performance of water based CuO and Al₂O₃ nanofluids in a Cu-Be alloy heat sink with rectangular microchannels. *Energy Convers Manag.* 2014;86:28–38.
50. Taylor R, Coulombe S, Otanicar T, Phelan P, Gunawan A, Lv W, et al. Small particles, big impacts: A review of the diverse applications of nanofluids. *J Appl Phys.* 2013;113(1):011301.
51. Huminc G, Huminc A. Application of nanofluids in heat exchangers: A review. *Renew Sustain Energy Rev.* 2012;16(8):5625–38.

52. Murshed SMS, Nieto de Castro CA, Lourenço MJV, Lopes MLM, Santos FJV. A review of boiling and convective heat transfer with nanofluids. *Renew Sustain Energy Rev.* 2011;15(5):2342–54.
53. Vajjha RS, Das DK. A review and analysis on influence of temperature and concentration of nanofluids on thermophysical properties, heat transfer and pumping power. *Int J Heat Mass Transf.* 2012;55(15):4063–78.
54. Sheikholeslami M, Seyednezhad M. Nanofluid heat transfer in a permeable enclosure in presence of variable magnetic field by means of CVFEM. *Int J Heat Mass Transf.* 2017;114:1169–80.
55. Tlili I, Bhatti M, Hamad SM, Barzinjy AA, Sheikholeslami M, Shafee A. Macroscopic modeling for convection of Hybrid nanofluid with magnetic effects. *Phys A.* 2019;534:122–36.
56. Cortes D, Santamarina J. Engineered soils: thermal conductivity; 2012.
57. Hosseini M, Sadri R, Kazi SN, Bagheri S, Zubir N, Bee Teng C, et al. Experimental Study on Heat Transfer and Thermo-Physical Properties of Covalently Functionalized Carbon Nanotubes Nanofluids in an Annular Heat Exchanger: A Green and Novel Synthesis. *Energy Fuels.* 2017;31(5):5635–44.
58. Ding Y, Alias H, Wen D, Williams RA. Heat transfer of aqueous suspensions of carbon nanotubes (CNT nanofluids). *Int J Heat Mass Transf.* 2006;49(1):240–50.
59. Fox EB, Visser AE, Bridges NJ, Amoroso JW. Thermophysical Properties of Nanoparticle-Enhanced Ionic Liquids (NEILs) Heat-Transfer Fluids. *Energy Fuels.* 2013;27(6):3385–93.
60. Wang X-j, Li X, Yang S. Influence of pH and SDBS on the Stability and Thermal Conductivity of Nanofluids. *Energy Fuels.* 2009;23(5):2684–9.
61. Amiri A, Sadri R, Ahmadi G, Chew BT, Kazi SN, Shanbedi M, et al. Synthesis of polyethylene glycol-functionalized multi-walled carbon nanotubes with a microwave-assisted approach for improved heat dissipation. *RSC Advances.* 2015;5(45):35425–34.
62. Duangthongsuk W, Wongwises S. Heat transfer enhancement and pressure drop characteristics of TiO₂–water nanofluid in a double-tube counter flow heat exchanger. *Int J Heat Mass Transf.* 2009;52(7):2059–67.
63. Amiri A, Shanbedi M, Rafieerad AR, Rashidi MM, Zaharinie T, Zubir MNM, et al. Functionalization and exfoliation of graphite into mono layer graphene for improved heat dissipation. *Journal of the Taiwan Institute of Chemical Engineers.* 2017;71:480–93.
64. Sarafraz MM, Yang B, Pourmehran O, Arjomandi M, Ghomashchi R. Fluid and heat transfer characteristics of aqueous graphene nanoplatelet (GNP) nanofluid in a microchannel. *Int Commun Heat Mass Transfer.* 2019;107:24–33.
65. Oon CS, Amiri A, Chew BT, Kazi SN, Shaw A, Al-Shamma'a A. Increase in convective heat transfer over a backward-facing step immersed in a water-based TiO₂ nanofluid. *Heat Transfer Research.* 2018;49(15):1419–29.
66. Zubir MNM, Muhamad MR, Amiri A, Badarudin A, Kazi SN, Oon CS, et al. Heat transfer performance of closed conduit turbulent flow: Constant mean velocity and temperature do matter! *Journal of the Taiwan Institute of Chemical Engineers.* 2016;64:285–98.
67. Oon CS, Badarudin A, Kazi SN, Fadhli M. Simulation of Heat Transfer to Turbulent Nanofluid Flow in an Annular Passage. *Adv Mater Res.* 2014;925:625–9.
68. Oon CS, Togun H, Kazi SN, Badarudin A, Sadeghinezhad E. Computational simulation of heat transfer to separation fluid flow in an annular passage. *Int Commun Heat Mass Transfer.* 2013;46:92–6.
69. Hosseini M, Abdelrazek AH, Sadri R, Mallah AR, Kazi SN, Chew BT, et al. Numerical study of turbulent heat transfer of nanofluids containing eco-friendly treated carbon nanotubes through a concentric annular heat exchanger. *Int J Heat Mass Transf.* 2018;127:403–12.
70. Silva VF, Batista LN, De Robertis E, Castro CSC, Cunha VS, Costa MAS. Thermal and rheological behavior of ecofriendly metal cutting fluids. *J Therm Anal Calorim.* 2016;123(2):973–80.
71. Kakaç S, Pramuanjaroenkij A. Review of convective heat transfer enhancement with nanofluids. *Int J Heat Mass Transf.* 2009;52(13):3187–96.
72. Xuan Y, Roetzel W. Conceptions for heat transfer correlation of nanofluids. *Int J Heat Mass Transf.* 2000;43(19):3701–7.
73. Sharma K, Sarm PK, Azmi WH, Mamat Rizalman, Kadirgama K. Correlations to predict friction and forced convection heat transfer coefficients of water based nanofluids for turbulent flow in a tube. *Int J Microscale Nanoscale Thermal Fluid Transp Phenom.* 2012;3(4):25.
74. Incropera FP. *Fundamentals of heat and mass transfer.* New York: Wiley; 2006.
75. Gnielinski V. On heat transfer in tubes. *Int J Heat Mass Transf.* 2013;63:134–40.

Publisher's Note Springer Nature remains neutral with regard to jurisdictional claims in published maps and institutional affiliations.